OPEN ACCESS

Large-scale steady-state structure of a 2D plasma crystal

New Journal of Physics
An Institute of Physics and Deutsche Physikalische Gesellschaft Journal

Large-scale steady-state structure of a 2D plasma crystal

S Zhdanov, R A Quinn, D Samsonov and G E Morfill
Max-Planck-Institute for Extraterrestrial Physics, 85748 Garching, Germany
E-mail: raq@mpe.mpg.de

New Journal of Physics **5** (2003) 74.1–74.11 (http://www.njp.org/)
Received 5 February 2003, in final form 1 May 2003
Published 17 June 2003

Abstract. An analytical model, based on a simple physical analogy, and a non-linear analytic/numerical model of the large-scale structure (averaged over the size of a single cell) of a two-dimensional (2D) lattice have been developed. In the first model, a physical analogy between the lattice layer steady state and the stressed state of a rotating solid body was used to derive the model equations and the model is shown to be in good agreement with the results of a 2D simulation. The non-linear model is derived from the force balance between external and internal forces in the continuum limit and compares favourably with an experimental example.

Contents

PII: S1367-2630(03)59254-0

1. Introduction

Numerous experiments with complex plasmas [1] have shown that the micrometre-sized particles in these plasmas:

(1) charge negatively and interact through a shielded Coulomb repulsion,
(2) are levitated and confined by electric fields near the edges of the plasma discharges, and
(3) form crystalline structures ('plasma crystals') under suitable experimental conditions.

Therefore, the large-scale spatial particle distribution should be governed by the distribution of the external force and the interparticle potential. With an appropriate model, it is hoped that measurements of the spatial particle distribution, which are relatively easy to obtain in plasma crystal experiments, will yield information about this external force and the interparticle potential. Significantly, these measurements can be obtained without external perturbation of the particle cloud or plasma.

Considering first the confinement fields, under gravity conditions a vertical electric field strong enough to levitate the particles is provided by the electrode sheath in typical discharge experiments. A model for the sheath electric field has been used in order to estimate experimentally the particle charge through observations of resonantly excited vertical oscillations of the grains [2, 3]. In these experiments, it was also proved that the neutral gas damping rate corresponds well to the Epstein drag coefficient. The neutral gas plays an important role in plasma crystal experiments by dissipating energy coupled to the particles through interactions with the background plasma.

The particles also experience a horizontal confinement. Experiments [4, 5] and simulations [6] predict that the horizontal confinement force should be weaker by 10–100 times compared with the vertical one. In this case, direct measurements (e.g. resonant oscillations) are difficult (but see [7] for another method) and the theory is not well developed. As we show below, however, the problem can be solved, at least for a rough potential distribution, averaged on a scale exceeding the size of the elementary crystal cell.

Partly due to the large ratio of the vertical to horizontal confining potentials, many experimental plasma crystals are two-dimensional (2D) or quasi-2D. Here, we consider single-layer 2D plasma crystals, taking no account of possible vertical motions of the particles. Such systems have been shown to display a Yukawa-type screened Coulomb interparticle potential [7, 5, 8]. Therefore, we use the Yukawa potential for the simulation results presented below.

Previous works in the field of complex plasmas have been devoted to an analysis of the macroscopic density distribution in experimental plasma crystals. For example, in [6] the authors constructed a functional for the intergrain potential energy and then minimized it to predict the macroscopic density profile. As discussed in [6], the 'local density approximation' (LDA) applies (strictly speaking) only to the short screening length case, $\lambda_D \ll a$, where a is the interparticle spacing and λ_D is the Debye screening length. It is worth noting that the LDA approach should also be applicable if the crystal size $R \gg \lambda_D$. Note also that the LDA should not be confused with the continuum limit; the latter is valid when $a \ll R$. This is practically always a good approximation for a cluster containing several hundreds of particles.

In [4], the authors constructed a model using an analysis of the local force balance. However, since the authors have included in the force balance only the interaction between two nearest grains, their approach also applies, in the formal limit, to $\lambda_D \ll a$. Most experimental results,

on the other hand, have been obtained under the conditions where $\kappa = a/\lambda_D \sim 0.5$–2 and the above-mentioned analytical models need to be extended to this interaction range, a task we undertake a first step towards here.

In the next section, we propose a model based on a simple physical analogy, developing it for a 2D cylindrically symmetric plasma crystal as well as a 1D planar system. This model is compared favourably with simulation results in section 3. In section 4, a non-linear model is developed and compared with experimental results in section 5. Both of these models take into account the effectively long-range nature (even for these screened Coulomb systems) of the interaction potential.

2. Simple model

We develop our simple model for the macroscopic density distribution n in a plasma crystal through an analogy with the stretched state of a solid cylinder rotating around its symmetry axis with a fixed angular velocity. The equation for the cylinder is [9]:

$$C_s^2 \nabla(\nabla \cdot \boldsymbol{u}) = -\Omega_{\text{rot}}^2 \boldsymbol{r} \tag{1}$$

where $\boldsymbol{u}$ is the displacement vector defined at each lattice site, C_s is the compressional sound speed defined in terms of the solid body elasticity modulus, and Ω_{rot} is the angular velocity of the rotation. The equation describing plasma crystal steady state can be written down immediately by analogy:

$$C_s^2 \nabla(\nabla \cdot \boldsymbol{u}) = \Omega^2 \boldsymbol{r} \tag{2}$$

where we have changed the sign on the right-hand side since the plasma crystal is compressed by the parabolic confinement potential. Now, C_s is the dust-lattice sound speed of the plasma crystal and Ω is the 'harmonic frequency' of the horizontal confinement (i.e. a dust grain having mass m has a potential energy $m\Omega^2 r^2/2$ in the confining field). Note that the right-hand side $\Omega^2 r$ is just the first non-zero term in the expansion of a general confinement force F_{ext}, assuming azimuthal symmetry.

Equation (2) can be formally derived in the same way as equation (1), i.e. by introducing the stretch modulus. Since this procedure is already well known, we use the simple physical analogy of a stretched rotating solid to illustrate the principles of the full derivation. Note that equations (1) and (2) are the *linear* elastic deformation relations while we have a *non-linear* system. Fortunately, however, near the crystal centre the deformations of the particle positions from the 'ideal' crystal case are small and the linear theory may, in a first approximation, be applied.

For a plasma crystal, C_s is given by the well-known relation [10]

$$C_s^2 = \left(\frac{Q^2}{m\lambda_D}\right) F(\kappa) \tag{3}$$

where Q and m are the charge and mass per grain and κ is defined above. The function $F(\kappa)$ is computed as a sum over individual grain positions for an ideal 2D lattice, and can be usefully fitted by the following expression:

$$F(\kappa) = 7.029 \exp(-2.0173 \ln(\kappa) - 0.131\,45\kappa - 0.037\,34\kappa^2). \tag{4}$$

Equation (4) fits with better than 0.5% accuracy for $\kappa < 5$, the range considered here (see figure 1).

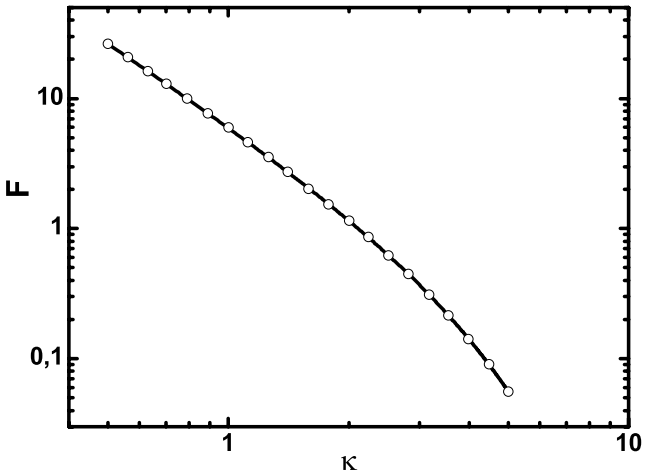

Figure 1. The κ dependence $F(\kappa)$ of the sound speed squared C_s^2 versus κ. The open circles give $F(\kappa)$ from the numerical summation, based on the results in [10], and the curve is the fit.

The next step is to obtain an expression for the density distribution in a lattice in terms of the displacements $\boldsymbol{u}$. Specifically, $\boldsymbol{u}$ represents the steady-state displacements of the particles in the plasma crystal from their ideal locations in a uniform 2D crystal. When the plasma crystal is treated as a continuous medium (see [11, 12] and section 4 below), the grain number density can be written:

$$\frac{n_0}{n} \approx 1 + \nabla \cdot \boldsymbol{u}, \tag{5}$$

where $n = n(r)$ is the spatial density distribution and n_0 is the density at the crystal centre. Equation (5) becomes an exact equality in the continuum limit, while here the approximate equality is due to coarse graining. Note also that $n = 2/(3^{1/2}a^2)$ for the perfect 2D triangular lattice. In this paper, we consider density changes on scales much larger than a.

2.1. Solution for the cylindrically symmetric case

Next we want to solve equations (2) and (5) for the cylindrically symmetric case. To do so, we first need to construct proper boundary conditions. Here, the analogy between the rotating solid body and the plasma crystal breaks down due to the different types of interparticle potentials: attractive–repulsive van der Waals type of interaction for the first but only repulsive for the second[1]. Hence, the boundary conditions can be different. For example, in the case of rotation-induced deformation, the surface of the solid body should be free from stresses [9]. Usually, it is assumed that the normal component of the stress tensor should be equal to zero on the surface and that the displacement should be finite throughout. Undoubtedly, the second condition should be fulfilled in the present case as well. However, the first does not apply for the present case, so we take as the second boundary condition $n = n_0$ at the crystal centre.

[1] This is strictly true for the case of a single-layer plasma crystal with no vertical motion. For multilayer plasma crystals, the ion-focus effect produces an additional attractive component for the interparticle interaction [14].

Applying these boundary conditions (finite density at $r = 0$ and $n_0/n = 1$ at $r = 0$) to equation (2), the solution is straightforward and takes the form

$$\boldsymbol{u} = u\boldsymbol{e}_r \qquad u = \frac{1}{8}\frac{\Omega^2 r^3}{C_s^2} \qquad \frac{\delta n}{n} \equiv \frac{(n_0 - n)}{n} \equiv \left(\frac{a}{a_0}\right)^2 - 1 = \frac{1}{2}\frac{\Omega^2 r^2}{C_s^2}. \tag{6}$$

According to equation (6), observation of the structure near the crystal centre immediately gives information on the confinement parameter, if the sound speed was found independently. For example, C_s can be found by analysing the naturally occurring phonon spectrum [13], or by shock or soliton propagation [11].

2.2. Solution for the 1D case

Under the action of non-symmetric external forces, and/or perturbing internal forces, such as chains of defects, the crystal structure may be approximately 1D planar (see [11] and below). Here, the density in the crystal varies primarily along the x direction. The solution is straightforward and, as in equation (6), one obtains

$$\left(\frac{a}{a_0}\right) - 1 = \frac{1}{2}\frac{\Omega^2 x^2}{C_s^2}. \tag{7}$$

3. Simulation results

To check our model, a molecular dynamics simulation was performed. The simulation consisted of a 2D crystal layer containing 721 particles, each having a charge of $Q = 16\,000e$ and interacting via a Yukawa-type (screened Coulomb) interparticle potential. The grain charge and screening length were kept constant during the simulation. The particles were confined by a cylindrically symmetric parabolic potential well and cooled by interaction with an Epstein-type drag force. The particles were placed randomly into the simulation box and the system was allowed to gradually approach equilibrium. The drag force was only sufficient to suppress numerical noise in the system and remove the initial kinetic energy. Finally, in equilibrium, the particles had a kinetic temperature of about 0.0001 eV. See [11] for further details about the simulation.

The equilibrium distribution is shown in figure 2, along with the Voronoi map for the lattice. The Voronoi map defines the set of points around each lattice site which are closer to that lattice cite than the surrounding nearest neighbours. This is also known as the Wigner–Seitz cell. The inverse of the area contained in a given Wigner–Seitz cell is a good approximation of the local area density in the lattice. Here, we compute the local interparticle spacing $a = (3a_W)^{1/2}/2$ where a_W is the Wigner–Seitz area.

The next step is to fit equation (6) to the simulation data and compare the resulting coefficients with the known values in the simulation. Rather than using it directly, we integrate equation (6) to obtain

$$N(r) = 2\pi \int n(r) r \, \mathrm{d}r = \left(\frac{\pi n_0}{k}\right) \ln(1 + kr^2) \tag{8}$$

where $N(r)$ is the radial distribution function and $k \equiv \Omega^2/(2C_s^2)$ is the fit coefficient. The function along with the fit is shown in figure 3. Note that the fit is good in the vicinity of the crystal centre and off towards the edge, as expected for regions where deformations and forces

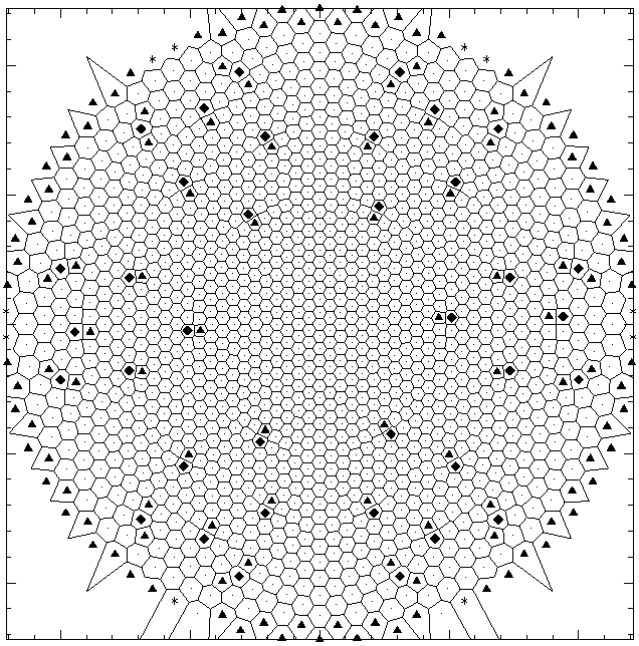

Figure 2. Particle distribution for a molecular dynamics simulation of a 2D plasma crystal along with a Voronoi map. All distances are measured in units of the screening length. The marked point is the geometric centre. The simulation parameters are: $Q = 16\,000e$, $\Omega = 2\ \mathrm{s}^{-1}$, $m = 5.5 \times 10^{-10}$ g, $\lambda_D = 750\ \mu$m, $\kappa_0 = 1.12$, $N = 721$.

are more non-linear, and we obtain $k_{\mathrm{fit}} = 0.31\ \mathrm{cm}^{-2}$. To judge the quality of our model, we compute a predicted k_{sim} from the known parameters of the simulation. Using the charge, mass, screening length and measured centre interparticle spacing a_0 in equations (3) and (4), we obtain $C_s = 2.57\ \mathrm{cm\ s}^{-1}$ and, with $\Omega = 2\ \mathrm{s}^{-1}$, $k_{\mathrm{sim}} = 0.30\ \mathrm{cm}^{-2}$. Therefore, $k_{\mathrm{sim}} \approx k_{\mathrm{fit}}$ within 3%.

As a further test of the simulation and of our model, a subsonic compression wave was launched through the simulation volume. The disturbance was tracked by computing the average density in the crystal as a function of time and space. The resulting pulse trajectory is shown in figure 4. Fitting the pulse-peak trajectory yields an estimate for the sound speed in the lattice, $C_{\mathrm{fit}} = 2.50\ \mathrm{cm\ s}^{-1}$. Note that this value is very close to that estimated above from the simulation parameters, as expected. Using this value in conjunction with our fitted value for k above yields an estimate for the confinement parameter, $\Omega = 1.97\ \mathrm{s}^{-1}$, in good agreement with the simulation value.

4. Non-linear model

While reasonably good at describing the equilibrium density distribution near the plasma crystal centre, the simple model proposed above fails in two ways: (1) the sound speed of an inhomogeneous crystal is position dependent ($C_s \equiv C_s(\kappa), \kappa \equiv \kappa(x)$), and (2) the grain displacement is actually large for large x. Here, we consider a 1D planar non-linear equation to describe the equilibrium density distribution.

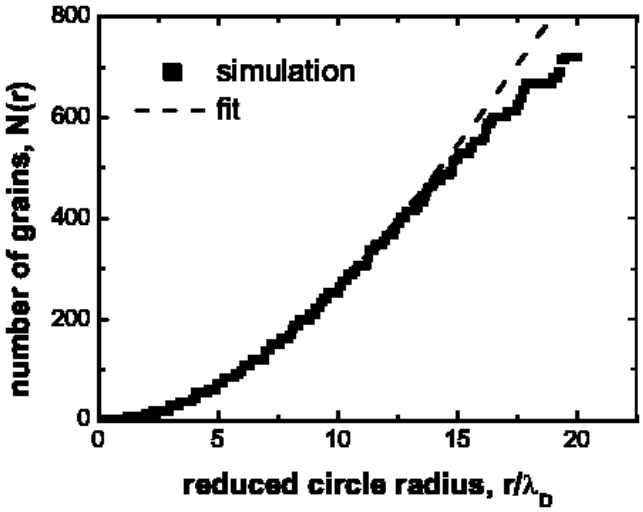

Figure 3. Radial distribution function $N(r)$ for the simulation data shown in figure 2. The dashed curve is the fit to equation (8). The fitted parameter is $k_{\text{fit}} = 0.31\ \text{cm}^{-2}$. Parameter $a_0 = 840\ \mu\text{m}$ was measured directly from the data and $n_0 = 2/(3^{1/2}a_0^2) = 1.63\ \text{mm}^{-2}$.

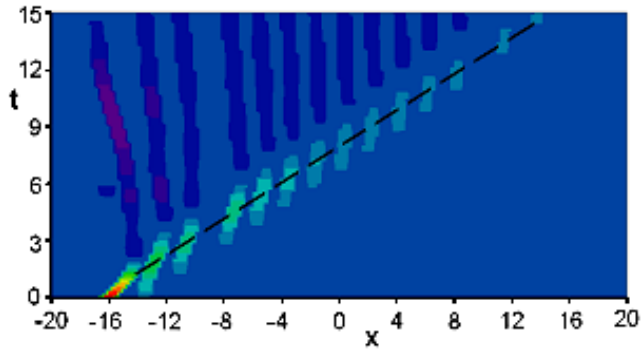

Figure 4. Trajectory of a subsonic compression pulse propagated in the simulation crystal shown in figure 2. The dashed line is a fit for the sound speed, $C_{\text{fit}} = 2.5\ \text{cm s}^{-1}$. The spatial scale in the plot is normalized to λ_D.

First, we rederive equation (5) for the 1D case, assuming uniform density in the direction perpendicular to x. Starting with an infinite homogeneous crystal, we cut a slice of thickness S_x from this crystal, perpendicular to the x axis. In the absence of external forces, the crystal will expand in x until it is destroyed. Suppose, however, that we stop the expansion by applying a symmetric external force which vanishes at the line of symmetry ($x = 0$) but grows with distance. This is the simplest interesting case and it is often realized in experiments. When the confining force is large enough, the slice can remain crystalline, but the particles will change their positions with respect to the initial state. The crystal is deformed.

To describe the deformation more precisely, consider a narrow element $\mathrm{d}x$ of the original (infinite) lattice at position x. The number of grains inside this element is $\mathrm{d}N = n_0 S_y\,\mathrm{d}x$. Here, n_0 is the grain number density per unit area before deformation, and S_y is the (constant) in-plane

width perpendicular to x. After deformation, this element occupies a new position $X = x + u$, where u is the displacement. Assume that the number of grains in this element remains the same ($\mathrm{d}N = nS_y\,\mathrm{d}X$), so that conservation of the grain number takes place. This is equivalent to assuming that no defects are generated through the deformation (the deformation is *elastic*). We then have

$$\frac{\mathrm{d}X}{\mathrm{d}x} = 1 + \frac{\mathrm{d}u}{\mathrm{d}x} = \frac{n_0}{n}, \tag{9}$$

equivalent to equation (5).

Now, if the forces acting on every element of a crystal layer are in balance, then the layer is in equilibrium. In the case of our deformation, the external forces should compensate a gradient of internal stresses: then the force balance can be written as

$$F_{\mathrm{ext}} = \frac{1}{n}\frac{\mathrm{d}p}{\mathrm{d}x}, \tag{10}$$

where F_{ext} is the external force acting on a given test grain at position x, and $n^{-1}\mathrm{d}p/\mathrm{d}x$ is the gradient of internal stresses (or 'pressure', by the terminology used in [4]) per grain. Assuming a parabolic confining well in X (the *equilibrium* coordinates), $F_{\mathrm{ext}} = -m\Omega^2 X$ and using the relation

$$C_s^2 = m^{-1}\frac{\partial p}{\partial n}, \tag{11}$$

equation (10) can be rewritten as

$$C_s^2\frac{1}{n}\frac{\mathrm{d}n}{\mathrm{d}x} = -\Omega^2 X. \tag{12}$$

Equations (3), (4), (9), (12) are the equations of the non-linear model describing the large-scale plasma crystal structure. Assuming a constant screening length λ_D, then we additionally have $\mathrm{d}X/\mathrm{d}x = n_0/n = a/a_0 = \kappa/\kappa_0$.

Note that equation (11) is valid if the internal stresses depend on the coordinates only indirectly via the crystal density coordinate dependence. It is not valid for the case of a crystal with defects. This has a very simple explanation: if a defect appears, it causes additional stresses in the crystal. The distribution of these stresses depends mainly on the spatial distribution of the defects, not just on the local crystal density. Here, we concentrate on weakly defected crystals, leaving the topic of particle distribution in defected crystals to another paper.

It is not too difficult to find a formally exact solution to the above set of non-linear equations. First, combining equations (9) and (12), we obtain

$$\Omega^2 X\frac{\mathrm{d}X}{\mathrm{d}x} = -C_s^2(\kappa)\frac{\mathrm{d}n}{\mathrm{d}x}\frac{n_0}{n^2}. \tag{13}$$

We have, on integrating,

$$\frac{1}{4}\Omega^2 X^2 = \int_n^{n_0}\mathrm{d}n\,\frac{n_0}{n^2}C_s^2 = \int_{\kappa_0}^{\kappa}\mathrm{d}\kappa\,\frac{C_s^2(\kappa)}{\kappa_0}. \tag{14}$$

This relation gives us the dependence $X = X(\kappa)$ needed for further integration, yielding

$$x = \int \mathrm{d}x = \int \mathrm{d}\kappa\left(\frac{\mathrm{d}\kappa}{\mathrm{d}x}\right)^{-1} = \int_{\kappa_0}^{\kappa}\mathrm{d}\kappa\,\frac{C_s^2(\kappa)}{\Omega^2\kappa X(\kappa)}. \tag{15}$$

Considering equation (4), the dependence of the sound speed on κ is too complicated in general to hope for a simple analytical result in integrating equations (14) and (15) above.

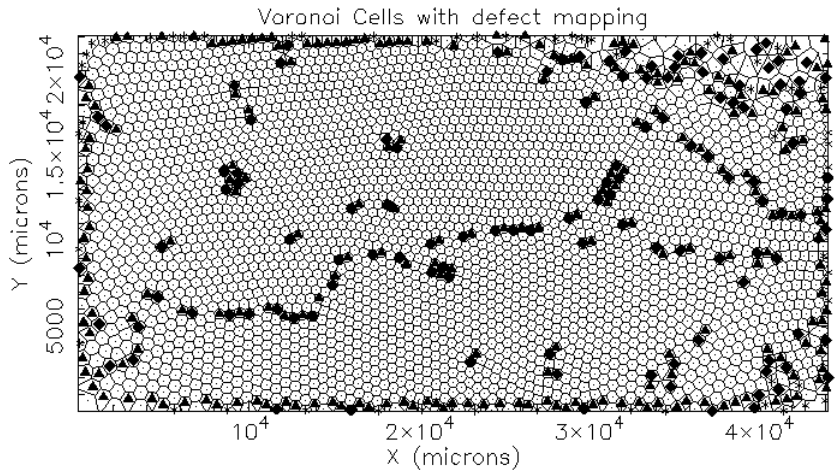

Figure 5. Experimentally observed crystalline structure. Particle positions are marked along with a Voronoi map. An electrically floating, horizontal wire was positioned about 2 cm to the right in this image.

Nevertheless, it is interesting to construct simple analytical, albeit approximate, results. To solve this problem, note that the plot in figure 1 is essentially linear for $\kappa < 1$, implying that $F(\kappa)$ has a power law dependence on κ in this regime. Referring again to equation (4), the dependence is approximately $F = F_0\kappa^{-2}$, with $F_0 =$ constant (see also [10]). Using this approximation, we obtain the following analytic solution:

$$\frac{x^2}{2L^2} = \Psi(a) \equiv \left(1 - \frac{a_0}{a}\right)\left(1 - \frac{1 - a_0/a}{3}\right)^2, \tag{16}$$

where $L = C_s(\kappa_0)/\Omega$. Note that this solution agrees well with equation (7) in the vicinity of $x = 0$. Equation (16) can be used to fit the observed crystal structure, to find the characteristic length L of the inhomogeneity. Then, the Ω confinement parameter can be computed after obtaining the crystal sound speed in a different experiment.

5. Experimental results

A particular example of an experimentally observed large-scale crystalline structure is shown in figure 5. It is a single-layer plasma crystal consisting of 6.5 μm grains embedded in the sheath of a low-pressure (1.8 Pa) rf plasma. A horizontal wire lies to the right of the area shown in figure 5. It was used to launch shock waves and solitons into the crystal. These results, as well as a complete description of the experiment, are presented in [11]. Stresses due to the wire induce defect formation in the equilibrium lattice and we suppose that these defects, along with the bulk deformation of the lattice due to the presence of the wire, are responsible for the 1D nature of the lattice deformation. Note that the lattice deformation becomes less 1D near the edges and we select only the central half of the image for further processing.

In order to obtain information about the effective confinement parameter, we start by computing $\Psi(a)$ (equation (16)) for the data shown in figure 5. First, we compute a_0 and $a(x)$ following the procedure described above in section 3. Next, we make a two-parameter fit using equation (16) ($x \to x - x_0$) to the experimentally determined $\Psi(a)$. This is shown in

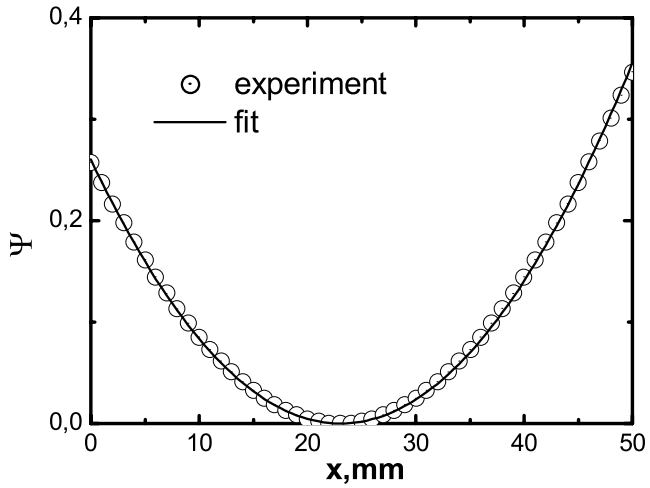

Figure 6. Computation of $\Psi(a)$ from equation (16) for the plasma crystal experiment of figure 5, along with fit. The fit yielded $x_0 = 23.1$ mm and $L = C_s/\Omega = 31.8$ mm.

figure 6. For the fit, we obtain $x_0 = 23.1$ mm and $L = C_s/\Omega = 31.8$ mm. The data are well described by the parabolic fit equation. From the results of the wave measurements performed in [11], we know that the sound speed in the lattice was $C_s \equiv C_s(\kappa_0) = 2.3 \pm 0.3$ cm s^{-1}. The corresponding estimate for the confinement parameter is then $\Omega = 0.7 \pm 0.4$ s^{-1}, where most of the error comes from the sound velocity measurement.

Assuming that Ω, Q and λ_D are constant in the vicinity of the crystal centre, it is possible to solve equations (14) and (15) numerically for different values of x_0, L and κ_0. The hope would be to obtain an additional fit to κ_0. However, it turns out that the fit is relatively insensitive to the value of κ_0, at least for the experiment tested here, in the range $0.5 < \kappa_0 < 2$.

6. Conclusion

Two models, one based on a simple analogy between a plasma crystal and a rotating rigid body that yields an analytic solution and a non-linear model based on a continuum description of the force balance, have been presented. The simple model describes well the equilibrium particle distribution for a simulated cylindrically symmetric 2D plasma crystal. The non-linear model, which yields an approximate analytic solution for κ less than about 2, was solved for the 1D case and used to fit an experimental distribution. In conjunction with data for the sound speed obtained in a separate wave propagation experiment, an estimate for the horizontal confinement parameter was obtained. Both models improve on previous work by taking into account the effect of having screening lengths of the order of the interparticle spacing, in line with previous experimental work in the field.

Acknowledgments

The authors gratefully acknowledge useful discussions with A V Ivlev and helpful comments from the referees. This work was supported by DLR/BMBF under grant nos PK-4 and 50WP0204.

References

[1] Thomas H *et al* 1994 *Phys. Rev. Lett.* **73** 652
[2] Homann A, Melzer A and Piel A 1999 *Phys. Rev.* E **59** R3835
[3] Ivlev A V *et al* 2000 *Phys. Rev. Lett.* **85** 4060
[4] Hebner G A *et al* 2001 *Phys. Rev. Lett.* **87** 235001
[5] Hebner G A *et al* 2002 *Phys. Rev.* E **66** 046407
[6] Totsuji H, Totsuji C and Tsuruta K 2001 *Phys. Rev.* E **64** 066402
[7] Konopka U, Morfill G E and Ratke L 2000 *Phys. Rev. Lett.* **84** 891
[8] Daugherty J E *et al* 1992 *J. Appl. Phys.* **72** 3934
[9] Landau L D and Lifschitz E M 1987 *Theory of Elasticity* (Moscow: Nauka)
[10] Peeters F M and Wu X 1987 *Phys. Rev.* A **35** 3109
[11] Samsonov D *et al* 2002 *Phys. Rev. Lett.* **88** 095004
[12] Zhdanov S K, Samsonov D and Morfill G E 2002 *Phys. Rev.* E **66** 026411
[13] Nunomura S *et al* 2002 *Phys. Rev. Lett.* **89** 035001
[14] Melandsø F 1997 *Phys. Rev.* E **55** 7495